

## PacBio assembly with Hi-C mapping generates an improved, chromosome-level goose genome

--Manuscript Draft--

<b>Manuscript Number:</b>	GIGA-D-20-00133R2	
<b>Full Title:</b>	PacBio assembly with Hi-C mapping generates an improved, chromosome-level goose genome	
<b>Article Type:</b>	Data Note	
<b>Funding Information:</b>	National Key R & D Program of China (2018YFD0500403)	Prof. Mingzhou Li
	National Natural Science Foundation of China (U19A2036)	Prof. Mingzhou Li
	National Natural Science Foundation of China (31772576)	Prof. Mingzhou Li
	National Natural Science Foundation of China (31802044)	Dr. Yan Li
	China Postdoctoral Science Foundation (2018M643514)	Dr. Yan Li
<b>Abstract:</b>	<p><b>Background:</b> The domestic goose is an economically important and scientifically valuable waterfowl; however, a lack of high-quality genomic data has hindered research concerning its genome, genetics, and breeding. As domestic geese breeds derive from both the swan goose ( <i>Anser cygnoides</i> ) and the graylag goose ( <i>Anser anser</i> ), we selected a female Tianfu goose for genome sequencing. We generated a chromosome-level goose genome assembly by adopting a hybrid <i>de novo</i> assembly approach that combined PacBio single-molecule real-time sequencing, high-throughput chromatin conformation capture mapping, and Illumina short-read sequencing.</p> <p><b>Findings:</b> We generated a 1.11 Gb goose genome with contig and scaffold N50 values of 1.85 Mb and 33.12 Mb, respectively. The assembly contains 39 pseudo-chromosomes (<math>2n = 78</math>) accounting for ca. 88.36% of the goose genome. Compared with previous goose assemblies, our assembly has more continuity, completeness, and accuracy; the annotation of core eukaryotic genes and universal single-copy orthologs has also been improved. We have identified 17,568 protein-coding genes (PCGs) and a repeat content of 8.67% (96.57 Mb) in this genome assembly. We also explored the spatial organization of chromatin and gene expression in the goose liver tissues, in terms of inter-pseudo-chromosomal interaction patterns, compartments, topologically associating domains, and promoter-enhancer interactions.</p> <p><b>Conclusions:</b> We present the first chromosome-level assembly of the goose genome. This will be a valuable resource for future genetic and genomic studies on geese.</p>	
<b>Corresponding Author:</b>	Mingzhou Li, Ph.D. Sichuan Agricultural University Chengdu, Sichuan CHINA	
<b>Corresponding Author Secondary Information:</b>		
<b>Corresponding Author's Institution:</b>	Sichuan Agricultural University	
<b>Corresponding Author's Secondary Institution:</b>		
<b>First Author:</b>	Yan Li	
<b>First Author Secondary Information:</b>		
<b>Order of Authors:</b>	Yan Li	

	Guangliang Gao
	Yu Lin
	Silu Hu
	Yi Luo
	Guosong Wang
	Long Jin
	Qigui Wang
	Jiwen Wang
	Qianzi Tang
	Mingzhou Li, Ph.D.
<b>Order of Authors Secondary Information:</b>	
<b>Response to Reviewers:</b>	<p>GigaScience em@editorialmanager.com</p> <p>Dear Hans Zauner Please find enclosed our revised manuscript, "PacBio assembly with Hi-C mapping generates an improved, chromosome-level goose genome (GIGA-D-20-00133)", which we would like to resubmit to GigaScience. We sincerely appreciate the very thoughtful and constructive comments from the editor(s). We have gone in detail through all the comments and believe that we have adequately addressed all their questions and concerns. We have made all the changes in the revised version of the manuscript, and our point-by-point responses to the editor's comments are given below. We trust that the revised manuscript now meets the standards required for publication in GigaScience. We look forward to hearing a positive response from you. Best regards Mingzhou Li Ph.D./Professor/ Address: Institute of Animal Genetics and Breeding, College of Animal Science and Technology, Sichuan Agricultural University, Chengdu 611130, China. E-mail: mingzhou.li@sicau.edu.cn</p> <p>Detailed responses to Editor(s) Below, our responses are in black, all revisions in the manuscript are marked in red using the word's track change.</p> <hr/> <p>Comment 1: Please include a citation to your new GigaDB dataset (including the DOI link) to your reference list, and cite this in the data availability section and elsewhere in the manuscript, where appropriate. The citation is: [xx] Li Y, Gao G, Lin Y, Hu S, Luo Y, Wang G et al. Supporting data for "PacBio assembly with Hi-C mapping generates an improved, chromosome-level goose genome" GigaScience Database. 2020. <a href="http://dx.doi.org/10.5524/100789">http://dx.doi.org/10.5524/100789</a>. In the data availability section, please write something along the lines, "Supporting data, including [data type 1], [data type 2] [etc] is available via the GigaScience repository, GigaDB [xx]". Response 1: In the data availability section (line 248 to 250), we added "The chromosome-level goose genome assembly, annotation files, and other supporting data are available via the GigaScience GigaDB database", and we cited the new GigaDB dataset in line 418 to 420.</p> <p>Comment 2: Do you have a picture of a representative of the goose hybrid used in your study (that can be published under a CC-BY open licence)? If you have a picture, please include this as Fig. 1, usually our "genome data note " authors show a representative of the organism/breed for illustration.</p>

	<p>Response 2: As the suggestion from editor (s), we supplied a new picture to represent the Tianfu goose as the Figure1, and reordered the sequence of the corresponding supplementary figures.</p> <p>Comment 3: Please also add the NCBI taxon ID for the species in the methods section. <a href="https://www.ncbi.nlm.nih.gov/taxonomy">https://www.ncbi.nlm.nih.gov/taxonomy</a> (If this particular hybrid does not have its own ID, please mention the NCBI taxon IDs of <i>A. anser</i> and <i>A. cygnoides</i>).</p> <p>Response 3: Tianfu goose is a Chinese local breed with many outstanding characteristics, such as excellent egg-laying performance, a fast growth rate, and strong adaptability. The goose belonging to <i>Anser cygnoides domesticus</i> (NCBI: txid381198). In line 74, we added the NCBI taxon ID (NCBI: txid381198).</p> <p>Comment 4: For bioinformatics software tools you used, please add RRIDs (Reserach Resource Identifiers) in the methods section for unique identification. You can find the RRIDs here: <a href="https://scicrunch.org/resources">https://scicrunch.org/resources</a>. For example, when you first mention BUSCO in the methods section, add the following RRID in this format: (BUSCO, RRID:SCR_015008).</p> <p>Response 4: In the manuscript and supplemental material files, we supplied RRIDs for most of software and marked the changes in red. However, we did not found the RRIDs for the TACO software (line 130 of the text) and the PSYCHIC software (line 86 of the supplemental material) using the website (<a href="https://www.ncbi.nlm.nih.gov/taxonomy">https://www.ncbi.nlm.nih.gov/taxonomy</a>) or google search engine.</p> <p>Moreover, we also made changes elsewhere in the text.</p> <p>1.In the List of abbreviations section, we revised the “Anser anser: <i>A. anser</i>” to “<i>A. anser</i>: <i>Anser anser</i>” in line 252. In line 253, we revised “<i>Anser cygnoides</i>: <i>A. cygnoides</i>” to “<i>A. cygnoides</i>: <i>Anser cygnoides</i>”.</p> <p>2.In line 285, we deleted the funding National Natural Science Foundation of China (31872335).</p>
<b>Additional Information:</b>	
<b>Question</b>	<b>Response</b>
Are you submitting this manuscript to a special series or article collection?	No
<p><b>Experimental design and statistics</b></p> <p>Full details of the experimental design and statistical methods used should be given in the Methods section, as detailed in our <a href="#">Minimum Standards Reporting Checklist</a>. Information essential to interpreting the data presented should be made available in the figure legends.</p> <p>Have you included all the information requested in your manuscript?</p>	Yes
<p><b>Resources</b></p> <p>A description of all resources used, including antibodies, cell lines, animals and software tools, with enough information to allow them to be uniquely</p>	Yes

<p>identified, should be included in the Methods section. Authors are strongly encouraged to cite <a href="#">Research Resource Identifiers</a> (RRIDs) for antibodies, model organisms and tools, where possible.</p> <p>Have you included the information requested as detailed in our <a href="#">Minimum Standards Reporting Checklist</a>?</p>	
<p><b>Availability of data and materials</b></p> <p>All datasets and code on which the conclusions of the paper rely must be either included in your submission or deposited in <a href="#">publicly available repositories</a> (where available and ethically appropriate), referencing such data using a unique identifier in the references and in the “Availability of Data and Materials” section of your manuscript.</p> <p>Have you have met the above requirement as detailed in our <a href="#">Minimum Standards Reporting Checklist</a>?</p>	<p>Yes</p>

# 1 PacBio assembly with Hi-C mapping generates an improved, chromosome-level goose genome

2 Yan Li<sup>1,†</sup>, Guangliang Gao<sup>1,2,†,\*</sup>, Yu Lin<sup>1,†</sup>, Silu Hu<sup>1</sup>, Yi Luo<sup>1</sup>, Guosong Wang<sup>1,3</sup>, Long Jin<sup>1</sup>, Qigui Wang<sup>2</sup>,  
3 Jiwen Wang<sup>1</sup>, Qianzi Tang<sup>1</sup>, Mingzhou Li<sup>1,\*</sup>

4  
5 <sup>1</sup>Institute of Animal Genetics and Breeding, College of Animal Science and Technology, Sichuan  
6 Agricultural University, Chengdu 611130, China;

7 <sup>2</sup>Institute of Poultry Science, Chongqing Academy of Animal Sciences, Chongqing 402460, China;

8 <sup>3</sup>Department of Animal Science, Texas A&M University, College Station 77843, United States of  
9 America

10 <sup>†</sup>These authors contributed equally to this paper.

11 \* Corresponding author(s): Guangliang Gao: [guanglianggaocq@hotmail.com](mailto:guanglianggaocq@hotmail.com); Mingzhou Li:  
12 [mingzhou.li@sicau.edu.cn](mailto:mingzhou.li@sicau.edu.cn).

## 13 Abstract

### 14 Background:

15 The domestic goose is an economically important and scientifically valuable waterfowl; however,  
16 a lack of high-quality genomic data has hindered research concerning its genome, genetics, and breeding.  
17 As domestic geese breeds derive from both the swan goose (*Anser cygnoides*) and the graylag goose  
18 (*Anser anser*), we selected a female Tianfu goose for genome sequencing. We generated a chromosome-  
19 level goose genome assembly by adopting a hybrid *de novo* assembly approach that combined PacBio  
20 single-molecule real-time sequencing, high-throughput chromatin conformation capture mapping, and  
21 Illumina short-read sequencing.

### 22 Findings:

23 We generated a 1.11 Gb goose genome with contig and scaffold N50 values of 1.85 Mb and 33.12

24 Mb, respectively. The assembly contains 39 pseudo-chromosomes ( $2n = 78$ ) accounting for ca. 88.36%  
25 of the goose genome. Compared with previous goose assemblies, our assembly has more continuity,  
26 completeness, and accuracy; the annotation of core eukaryotic genes and universal single-copy orthologs  
27 has also been improved. We have identified 17,568 protein-coding genes (PCGs) and a repeat content of  
28 8.67% (96.57 Mb) in this genome assembly. We also explored the spatial organization of chromatin and  
29 gene expression in the goose liver tissues, in terms of inter-pseudo-chromosomal interaction patterns,  
30 compartments, topologically associating domains, and promoter-enhancer interactions.

### 31 **Conclusions:**

32 We present the first chromosome-level assembly of the goose genome. This will be a valuable  
33 resource for future genetic and genomic studies on geese.

34 **Key Words:** goose genome, chromosome-length assembly, hybrid *de novo* assembly approaches,  
35 annotation, Pacbio, Hi-C

36

## 37 **Data description**

### 38 **Context**

39 The goose is a member of the family Anatidae and is an economically important waterfowl with  
40 distinctive characters. Domesticated geese derive from the swan goose (*Anser cygnoides*) and the graylag  
41 goose (*Anser anser*)<sup>1</sup>, and approximately 6,000 years of artificial selection have led to significant  
42 alterations in their body size, reproductive performance, egg production, feather color, and other features<sup>2</sup>.  
43 Currently, more than 181 domesticated breeds are reared globally to supply meat, eggs, and valuable  
44 byproducts (feathers, fatty liver) for human consumption<sup>2,3,4</sup>. The domestic goose is also well suited to  
45 sustainable production practices because fiber can form part of its diet, which then lessens competition  
46 for human food<sup>5</sup>. Its excellent disease resistance and behavioral patterns also allow for large-scale

47 farming and easy management<sup>6</sup>. Interestingly, despite the liver weight of goose increasing 5–10 times  
48 after two to three weeks of overfeeding, the amount of fat in hepatic cells (and other biomedical  
49 parameters) returns to normal levels when overfeeding ceases. This suggests that the goose liver could  
50 provide a novel animal model for the study of human non-alcoholic fatty liver disease<sup>6</sup>.

51 The goose was one of the earliest animals to be domesticated<sup>2,7</sup>, and wide-ranging genomic and  
52 breeding research has been conducted to study its domestication process and the unique morphological  
53 and physiological features of these animals. For example, recently published goose genome sequences  
54 have been assembled into scaffolds using short reads from the Illumina platform<sup>8,9</sup>; however, the genetic  
55 basis of the fatty liver of goose and their selective breeding remains largely unknown. To address such  
56 issues, a high-quality genome sequence is required. Currently, there are many advantages to using hybrid  
57 *de novo* assembly approaches to improve the quality of genome assemblies. This is because short,  
58 accurate reads from the Illumina platform can be combined with the longer, less accurate reads generated  
59 by the single-molecule real-time (SMRT) sequencing platform<sup>10</sup>. With Hi-C, linking information can  
60 then be ordered and oriented into scaffolds, after which assembly errors can be identified and corrected<sup>11</sup>.  
61 This approach has been applied to improve the genome assemblies of many species, including humans<sup>12</sup>,  
62 goats<sup>13</sup>, rockfish<sup>14</sup>, *Aedes aegypti*<sup>11</sup>, and barley<sup>15</sup>.

63 Here, we have generated a chromosome-level goose assembly with chromosome-length scaffolds  
64 by adopting a hybrid *de novo* assembly approach using a combination of short reads from the Illumina  
65 platform, long reads from the PacBio platform, and Hi-C-based chromatin interaction maps. Our  
66 chromosome-level goose genome comprises longer scaffolds than currently available goose genome  
67 assemblies, and these scaffolds are of a higher-quality and are more continuous and accurate. Our new  
68 genome assembly thus provides a valuable resource for exploring the molecular basis of the

69 morphological and physiological features of the goose, and will facilitate further genomic, genetic, and  
70 breeding studies of this domesticated waterfowl.

## 71 **Methods**

### 72 **a) Sample collection and sequencing**

73 We extracted genomic DNA from the liver tissue of a healthy adult female (136 days old) from the  
74 Tianfu goose maternal line (NCBI: txid381198), which was provided by the Experimental Farm of  
75 Waterfowl Breeding of Sichuan Agricultural University (Chengdu, Sichuan, China; **Figure 1**). We then  
76 carried out single-molecule real-time DNA sequencing of ca. 20-kb inserts using the PacBio Sequel  
77 platform. This yielded approximately 84.31 Gb of high-quality sequencing data that were used to initially  
78 assemble the genome (**Table 1**). Next, 149.70 Gb of high-quality sequencing data were generated from  
79 a 350-bp insert size Hi-C library, as previously reported<sup>13</sup>. Finally, 350-bp paired-end libraries  
80 constructed from the same genomic DNA were sequenced on the Illumina HiSeq platform, producing a  
81 further 181.52 Gb of sequence data. In total, we obtained approximately 415.53 Gb sequencing data (ca.  
82 324.63× coverage) for our chromosome-level goose genome assembly (**Table 1**).

### 83 **b) *De novo* assembly of the goose genome**

84 The size of the goose genome was estimated by k-mer distribution analysis to be 1.28 Gb. To  
85 assemble the genome, we first performed an initial assembly with the PacBio long-reads alone, using  
86 Falcon (Falcon, RRID:SCR\_016089)<sup>16</sup> software. We used the pbsmrtpipe pipeline of the smrtlink  
87 (smrtlink, RRID:SCR\_002942) software to assemble the genome sequence, which resulted in a draft  
88 assembly with a contig N50 of 1.72 Mb (**Table S1**). Next, we used the single-molecule sequence reads  
89 to scaffold these contigs and fill gaps, using SSPACE-Long (SSPACE-Long, RRID:SCR\_005056)<sup>17</sup> and  
90 PBJelly (PBJelly, RRID:SCR\_012091)<sup>18</sup>, respectively. Pilon (Pilon, RRID:SCR\_014731)<sup>19</sup> software was



91 then used to map the short reads to the assembly (**Table S1**). Finally, 39 pseudo-chromosomes were  
92 assembled with the Hi-C reads were aligned using Lachesis ([Lachesis, RRID:SCR\\_017644](#))<sup>20</sup> software  
93 (**Table S2, Figure S1**); this is consistent with the number of goose chromosomes ( $2n = 78$ ) reported in  
94 previous studies<sup>21</sup>. With these methods, we generated a chromosome-level goose assembly with a contig  
95 N50 of 1.85 Mb and scaffold N50 of 33.12 Mb (**Table 2**). The average GC content is 42.15% and the  
96 total genome size is 1.11 Gb, which is consistent with previous studies<sup>8,9</sup> and suggests that our goose  
97 assembly is reliable.

### 98 **c) Repeat sequence and gene annotation**

99 *De novo* methods and homology-based approaches were used to annotate the repeat content of the goose  
100 genome. First, we used *ab initio*-prediction software, including LTR-finder ([LTR-finder,](#)  
101 [RRID:SCR\\_005659](#))<sup>22</sup>, RepeatMolder <sup>2</sup>([RepeatMolder, RRID:SCR\\_015027](#))<sup>3</sup>, and RepeatScout  
102 ([RepeatScout, RRID:SCR\\_014653](#))<sup>24</sup>, to perform *de novo* annotation of the genome. For homology-  
103 based predictions, we identified repeat regions across species in published RepBase sequences<sup>25</sup> using  
104 RepeatMasker ([RepeatMasker, RRID:SCR\\_012954](#))<sup>26</sup> and RepeatProteinMask ([RepeatProteinMask,](#)  
105 [RRID:SCR\\_012954](#))<sup>27</sup> software. Combined with these results, the repeat region of the goose genome  
106 was further predicted with RepeatMasker software. From these analyses, we identified 92.11 Mb of  
107 repetitive DNA (**Table S3**) accounting for 8.67% of our assembly, which is much higher than has been  
108 reported in previous studies<sup>8,9</sup>. Long interspersed nuclear elements (LINEs) were the most abundant  
109 repeat element identified, representing 6.83% of the genome. The proportion of LINE repetitive  
110 sequences identified in this study was also higher than has been reported in two previous goose genome  
111 assemblies (**Table S3**). We performed PCGs annotation by combining *ab initio*-based, homology-based,  
112 and RNA-sequencing-based prediction methods. First, GenScan ([GenScan, RRID:SCR\\_012902](#))<sup>28</sup>,

113 Geneid (Geneid, RRID:SCR\_002473)<sup>29</sup>, and Augustus (Augustus, RRID:SCR\_008417)<sup>30</sup> were used for  
114 *ab initio*-based predictions. Next, we selected six chromosome-level genomes, namely *Homo sapiens*  
115 (GCF\_000001405.39), *Mus musculus* (GCF\_000001635.26), *Gallus gallus* (GCF\_000002315.6), *Anas*  
116 *platyrhynchos* (GCF\_003850225.1), *Meleagris gallopavo* (GCF\_000146605.3), and *Taeniopygia*  
117 *guttata* (GCF\_003957565.1), to use for homology-based annotation of our goose chromosome-level  
118 assembly genome using TBLASTN (TBLASTN, RRID:SCR\_011822)<sup>31</sup> and GeneWise (GeneWise,  
119 RRID:SCR\_015054)<sup>32</sup> software. We found 8,255 common orthologous groups across these seven  
120 species (Figure S2). To optimize genome annotation, total RNA was extracted from 11 samples  
121 (abdominal fat, brain, duodenum, heart, liver, lung, muscular stomach, ovary, pancreas, pectoral muscle,  
122 and spleen) taken from the same individual whose DNA was used for the chromosome-level genome  
123 assembly. We pooled equal amounts of the total RNA from each of the 11 tissues and then performed  
124 RNA-seq on this pooled sample using the Illumina platform. After filtering, these data were used to  
125 annotate protein-coding regions of the genome assembly using Trinity (Trinity, RRID:SCR\_013048)<sup>33</sup>  
126 and TopHat (TopHat, RRID:SCR\_013035)<sup>34</sup>. Finally, the predictions from each method described above  
127 were integrated using EVM (EVM, RRID:SCR\_014659)<sup>35</sup>; overall, 17,568 PCGs were predicted (Table  
128 3, Figure S3). To identify long noncoding RNAs (lncRNAs), the goose genome reads were aligned by  
129 STAR (STAR, RRID:SCR\_015899)<sup>36</sup> and subjected to Cufflinks (Cufflinks, RRID:SCR\_014597)<sup>37</sup> and  
130 TACO<sup>38</sup> for assembly and filtering. CPC2(CPC2, RRID:SCR\_002764)<sup>39</sup> was then applied to perform  
131 coding potential analysis, and PfamScan (PfamScan, RRID:SCR\_004726)<sup>40</sup> was used to check for  
132 domain hits against Pfam31-A<sup>41</sup>. After removing all likely domains, 3,287 lncRNAs only by *ab initio*  
133 assembly method and 542 transcripts of uncertain coding potential (TUCP) were identified, the long  
134 reads will be helpful to improve the identification and annotation of the lncRNA and TUCP in goose

135 genome.

## 136 **Data validation and quality control**

### 137 **a) Assessment of genome assembly completeness**

138 Our assembly has more scaffolds and fewer contigs, and significantly improved contig and scaffold  
139 N50 values, than the goose genome assemblies presented in two previous studies (**Figure 2**). Moreover,  
140 we have annotated more repeat (Table S3) and exons sequence regions (Table 3) than these previous  
141 studies (**Table 3**), which suggests that we have generated an improved genome assembly and annotation.  
142 The 39 pseudo-chromosomes described in our study account for 88.36% of the assembled genome and  
143 are longer than those previously reported<sup>8,9</sup>, again indicating that our chromosome-level goose genome  
144 represents a significant improvement on previous work. The GC content of our genome assembly is 42%  
145 and the size of the genome is 1.11 Gb (**Table 2**). This is comparable to the sizes reported for the two  
146 previously constructed goose genomes<sup>8,9</sup> and is characteristic of avian genomes<sup>42</sup>. We also mapped short-  
147 insert paired-end reads (350 bp) to our chromosome-level goose genome and obtained mapping and  
148 coverage rates of 97.25% and 99.71%, respectively. Finally, we downloaded 19 wild goose  
149 resequencing<sup>43</sup> datasets from public databases and mapped them to our assembly, and to the two earlier  
150 draft goose genomes. We found that the mapping rate of our chromosome-level goose assembly was  
151 higher than that of the previously assembled genomes (**Table S4**), indicating that it is more contiguous.  
152 Taken together, these results demonstrate the improvements made by our study in the assembly and  
153 annotation of the goose genome, in comparison to previous studies<sup>8,9</sup>.

154 To evaluate the completeness of our chromosome-level genome assembly, we determined the  
155 number of conserved eukaryotic and universal genes present in our assembly by applying the core  
156 eukaryotic genes mapping approach software (**CEGMA, RRID:SCR\_015055**) and using a set of

157 benchmarking universal single-copy orthologs (BUSCO, RRID:SCR\_015008). We found that 211 of the  
158 248 (85.08%) core eukaryotic genes and 2,586 (97%) of the universal single-copy orthologs were  
159 assembled in our genome. Compared with previous studies, this suggests that our genome assembly is  
160 more complete than previous drafts of the goose genome<sup>8,9</sup>.

161 To explore the hypothesis that the leptin gene was lost from goose<sup>8</sup>, we downloaded leptin sequences  
162 from avian and mammal genomes to use as reference sequences in BLASTP (BLASTP,  
163 RRID:SCR\_001010) searches of our newly assembled goose genome. We found no sequences similar to  
164 leptin in our chromosome-level goose assembly. Furthermore, although the human genome region that  
165 contains the leptin gene (chromosome 7, 126.0 to 129.4 Mb) aligned with the goose genome, we did not  
166 find a sequence similar to the leptin gene in this region. These results confirm the previous finding that  
167 the leptin gene is not present in the goose genome<sup>8</sup>.

## 168 **b) Phylogenetic tree and lineage-specific gene families**

169 Using OrthoMCL (OrthoMCL, RRID:SCR\_007839)<sup>44</sup>, 16,157 orthologous gene families across 17  
170 species (ostrich, duck, goose, chicken, turkey, saker, red-legged seriema, African crowned crane, pelican,  
171 little egret, crested ibis, cormorant, great crested grebe, pigeon, woodpecker, zebra finch, and lizard)  
172 were identified. Based on 2,389 shared single-copy ortholog gene clusters, we constructed a maximum  
173 likelihood phylogenetic tree using the RAxML software (RAxML, RRID:SCR\_006086)<sup>45</sup>. This revealed  
174 that goose and duck diverged about 31.60 million years ago (Mya), which is comparable to the  
175 divergence time of chicken and turkey (32.33 Mya; **Figure S4**) and consistent with the previous studies  
176 <sup>18, 91</sup>. We also noted that lineage-specific genes in the goose genome were significantly enriched for  
177 olfactory receptor activity (GO:0004984,  $p = 3.85 \times 10^{-24}$ ), G protein-coupled receptor activity  
178 (GO:0004930,  $p = 6.67 \times 10^{-13}$ ), and integral component of membrane (GO:0016021,  $p = 0.01$ ; **Table S5**).

179 As a migratory bird, the goose is adapted for long-distance migration, which exposes them to a diversity  
180 of food as they seek out ideal habitats. We propose that such influences might strengthen the interactions  
181 between odorants and the receptors of the olfactory mucosa, and could underlie receptor family evolution  
182 in the goose genome.

### 183 **c) Expansion and contraction of gene families**

184 The expansions and contractions of gene clusters in the goose genome were identified in comparison  
185 to nine other avian genomes using the CAFE program (CAFÉ, RRID:SCR\_018924)<sup>46</sup>. We found 839  
186 expanded gene families (Table S6) and 2,193 contracted gene families (Table S7). Interestingly, the  
187 expanded gene families were mainly enriched for olfactory receptor activity (GO:0004984,  $p =$   
188  $8.58 \times 10^{-51}$ ), G protein-coupled receptor activity (GO:0004930,  $p = 5.81 \times 10^{-25}$ ), and integral component  
189 of membrane (GO:0016021,  $p = 3.20 \times 10^{-6}$ ), which is consistent with the results from our analysis of  
190 lineage-specific genes (Table S5). This further confirms that the migratory adaptations of the goose are  
191 reflected by unique characteristics in the goose genome that contrast with those of nonmigratory birds.  
192 Other expanded gene families were enriched for ATPase-coupled transmembrane transporter activity  
193 (GO:0042626,  $p = 1.96 \times 10^{-06}$ ), NAD(P)<sup>+</sup>-protein-arginine ADP-ribosyl transferase activity  
194 (GO:0003956,  $p = 3.20 \times 10^{-04}$ ), ATPase activity (GO:0016887,  $p = 8.28 \times 10^{-05}$ ), and aspartic-type  
195 endopeptidase activity (GO:0004190,  $p = 9.63 \times 10^{-06}$ ; Table S6), while gene families contracted in the  
196 goose were significantly enriched for transmembrane transport (GO:0055085,  $p = 8.30 \times 10^{-04}$ ), ion  
197 channel activity (GO:0005216,  $p = 1.87 \times 10^{-9}$ ), ion transmembrane transport (GO:0034220,  $p =$   
198  $5.30 \times 10^{-6}$ ), and ATPase-coupled intramembrane lipid transporter activity (GO:0140326,  $p = 8.60 \times 10^{-10}$ ;  
199 Table S7). As these pathways are related to ATP utilization, ATP production, and energy regulation, these  
200 data support a previous finding that goose energy metabolism is different from that in other avian

201 species<sup>47</sup>. This feature of the goose is possibly related to its migratory habits and artificial selection—  
202 the goose is unique among migratory birds because of its large body size, which requires much energy  
203 for long-distance, high altitude flying<sup>48</sup>.

#### 204 **d) Genes under positive selection**

205 We identified 52 positively selected genes (PSGs) in the goose genome based on orthologous genes  
206 from the 17 species above, using a branch-site model and F3x4 codon frequencies in [Codeml \(Codeml, RRID:SCR\\_004542\)](#) (Table S8). Some of these PSGs, such as *GCHI* (GTP-cyclohydrolase I), are  
207 associated with parkinsonism, dystonia, and phenylketonuria disease in humans<sup>49, 50</sup>. They also play a  
208 role in adaptation to high-altitude environments in humans, where they relate to a lower hemoglobin  
209 level, nitric oxide concentration, and oxygen saturation in the blood. Furthermore, previous studies have  
210 shown *GCHI* divergence between human populations living at different altitudes<sup>51</sup>. Selection acting on  
211 *GCHI* in goose is likely to be related to their adaptation to high-altitude or migratory habitats. *SNWI*  
212 (*SNWI* Domain Containing 1) is involved in the Nuclear Factor Kappa B pathway and is associated with  
213 oculopharyngeal muscular dystrophy disease<sup>52, 53</sup>. The depletion of this gene in breast cells leads to the  
214 induction of apoptosis, while the overexpression of this gene impedes neural crest development<sup>54</sup>.  
215 Selection acting on *SNWI* in goose suggests that it may confer protection from diseases and aid  
216 adaptation in changeable environments. *POU2F3* is pivotal in the discrimination of taste qualities, such  
217 as sweet, umami and bitter characteristics. Deficiency in this gene in mice alters their electrophysiology  
218 and behavioral responses to taste characters<sup>55, 56</sup>. Selection acting on *POU2F3* in goose is likely to be  
219 related to a requirement for seeking food in variable migratory habitats.

#### 221 **e) Initial characterization of the three-dimensional organization of goose liver tissues**

222 We analyzed the inter-pseudo-chromosomal interaction pattern<sup>57</sup>, compartments<sup>58, 59</sup>, topologically

223 associating domains (TADs)<sup>60</sup>, and promoter-enhancer interactions (PEI)<sup>61</sup> of the goose liver tissue. The  
224 matrix resolution of our Hi-C experiment reached ~2 Kb (defined as the smallest locus size such that 80%  
225 of loci have at least 1,000 contacts) (**Figure S5**), which was adequate for subsequent analyses of the  
226 chromatin architecture. Our results showed that the whole inter-pseudo-chromosomal interaction pattern  
227 was distinguished by two clusters, that is, short pseudo-chromosomes and longer pseudo-chromosomes,  
228 which suggests that goose pseudo-chromosomes tend to interact with one another on the basis of size  
229 (**Figure 3**). As for the identification of A and B compartments, which represent relatively active and  
230 inactive chromatin states, respectively, the number of protein-coding genes (PCGs) in each 100 Kb bin  
231 with at least 50 % percentage overlapped with a gene was counted. The number of PCGs was  
232 significantly correlated with PC1 values ( $R = 0.39$ ,  $p = 2.2 \times 10^{-16}$ ; **Figure S6**), and the transcripts per  
233 kilobase millions (TPMs) of PCGs located in A compartments were consistently higher than PCGs in B  
234 compartments in three liver tissues ( $p = 2.2 \times 10^{-16}$ ; **Figure S7, Table S9**). We identified 734 TADs across  
235 the goose assembly, accounting for 80% of the genome (**Figure S8, Table S10**). The mean and median  
236 sizes of the TADs were 1.21 Mb and 1.00 Mb, respectively. We also observed that the TSSs of PCGs  
237 were enriched in TAD-boundary regions (**Figure S9**). After filtering for interaction distances lower than  
238 20 Kb, we identified 13,017 PEIs (**Table S11**) and found that gene expression levels positively correlated  
239 with the number of its associated enhancers in all three liver tissues (**Figure S10**). This is suggestive of  
240 additive effects of enhancers on target-gene transcription levels.

#### 241 **Availability of supporting data**

242 The chromosome-level goose genome assembly sequence is available at National Center for  
243 Biotechnology Information (NCBI) GenBank through the accession number WTSS000000000; The high-  
244 quality Hi-C data are available through the NCBI Sequence Read Archive (SRA) database under

245 accession number SRR10483522. The PacBio long-read sequencing data have been deposited in the  
246 NCBI SRA (SRR10483521). The high-quality Illumina short-read sequencing data are available through  
247 NCBI SRA accession number: SRR10483516, SRR10483517, SRR10483518 and SRR10483520. The  
248 transcriptome data are available through the NCBI SRR10483519. **The chromosome-level goose genome  
249 assembly, annotation files, and other supporting data are available via the *GigaScience* GigaDB database  
250 <sup>62</sup>.**

## 251 **List of abbreviations**

- 252 (1) **A. anser**: *Anser anser*;
- 253 (2) **A. cygnoides**: *Anser cygnoides*;
- 254 (3) BUSCO: Benchmarking Universal Single-Copy Orthologs;
- 255 (4) CHMP1B: charged multivesicular body protein 1B;
- 256 (5) CEGMA: Core Eukaryotic Genes Mapping Approach software;
- 257 (6) TUCP: transcripts of uncertain coding potential;
- 258 (7) GCH1: GTP cyclohydrolase 1;
- 259 (8) Hi-C, Chromosome conformation capture;
- 260 (9) IVNS1ABP: influenza virus NS1A binding protein;
- 261 (10) LINES: Long interspersed nuclear elements;
- 262 (11) LncRNAs: long noncoding RNAs;
- 263 (12) OGFOD2: 2-oxoglutarate and iron dependent oxygenase domain containing 2
- 264 (13) MDH257: malate dehydrogenase 2
- 265 (14) PCGs: protein coding genes
- 266 (15) PEI: promoter-enhancer interactions;
- 267 (16) PSGs: positively selected genes;
- 268 (17) SMRT: single-molecule real-time;
- 269 (18) TADs: topological associated domains;
- 270 (19) TPMs: transcripts per kilobase millions.
- 271



272 **Ethics approval**

273 All animal experiments were approved and reviewed by Animal Care and Use Committee  
274 Institutional of Sichuan Agricultural University (Approval No. DKY-B20121406) and the Ministry of  
275 Science and Technology of the People's Republic of China (Approval No. 2006–398).

276

277 **Competing interests**

278 The authors declare no competing interest.

279

280 **Acknowledgments**

281 This work was supported by grants from the National Key R & D Program of China  
282 (2018YFD0500403), the National Natural Science Foundation of China (U19A2036, [31872335](#),  
283 31772576 and 31802044) and the China Postdoctoral Science Foundation (2018M643514).

284 **Author contributions**

285 Mingzhou Li, Guangliang Gao designed and supervised the project. Yan Li, Yu Lin, Qianzi Tang,  
286 Silu Hu performed bioinformatics analyses. Jiwen Wang, Yan Li and Yi Luo contributed to collect the  
287 samples. Mingzhou Li, Qigui Wang, Guangliang Gao, Yi Luo and Long Jin were involved in the data  
288 analyses and wrote the manuscript.

289

290 **References**

- 291 1. Shi XW, Wang JW, Zeng FT, et al. Mitochondrial DNA cleavage patterns distinguish independent  
292 origin of Chinese domestic geese and western domestic geese. *Biochem Genet.* 2006; 44(5-6) : 237-  
293 245.
- 294 2. Kozák J. Variations of geese under domestication. *World's Poult Sci J.* 2019; 75(2): 247-260.

- 295 3. Goluch-Koniuszy Z, Haraf G. Geese for slaughter and wild geese as a source of selected mineral  
296 elements in a diet. *J Elementol.* 2018; 23: 1343-1360.
- 297 4. Janan J, Tóth P, Hutas I, et al. Effects of dietary micronutrient supplementation on the reproductive  
298 traits of laying geese. *Acta Fytotech Zootech.* 2015; 18(1) : 6-9.
- 299 5. Zhang Y, Sha Z, Guan F, et al. Impacts of geese on weed communities in corn production systems  
300 and associated economic benefits. *Biol Control.* 2016. 99: 47-52.
- 301 6. Wang G, Jin L, Li Y, et al. Transcriptomic analysis between Normal and high-intake feeding geese  
302 provides insight into adipose deposition and susceptibility to fatty liver in migratory birds. *BMC*  
303 *genomics.* 2019; 20(1): 372.
- 304 7. Honka J, Heino M, Kvist L, et al. Over a thousand years of evolutionary history of domestic geese  
305 from Russian archaeological sites, analysed using ancient DNA. *Genes.* 2018; 9(7): 367.
- 306 8. Lu L, Chen, Y, Wang Z, et al. The goose genome sequence leads to insights into the evolution of  
307 waterfowl and susceptibility to fatty liver. *Genome Biol.* 2015; 16(1): 89.
- 308 9. Gao G, Zhao X, Li Q, et al. Genome and metagenome analyses reveal adaptive evolution of the host  
309 and interaction with the gut microbiota in the goose. *Sci Rep.* 2016; 6: 32961.
- 310 10. Schadt E, Turner S, Kasarskis A. A window into third-generation sequencing. *Hum Mol Genet.*  
311 2010; 19(R2): R227-R240.
- 312 11. Dudchenko O, Batra SS, Omer AD, et al. *De novo* assembly of the *Aedes aegypti* genome using  
313 Hi-C yields chromosome-length scaffolds. *Science.* 2017; 356(6333): 92-95.
- 314 12. Pendleton M, Sebra R, Pang AWC, et al. Assembly and diploid architecture of an individual human  
315 genome via single-molecule technologies. *Nat Methods.* 2015; 12(8): 780–786.
- 316 13. Bickhart DM, Rosen BD, Koren S, et al. Single-molecule sequencing and chromatin conformation

- 317 capture enable *de novo* reference assembly of the domestic goat genome. Nat Genet. 2017; 49(4):  
318 643.
- 319 14. Liu Q, Wang X, Xiao Y, et al. Sequencing of the black rockfish chromosomal genome provides  
320 insight into sperm storage in the female ovary. DNA Research, 2019. 26(6):453–464,
- 321 15. Mascher M, Gundlach H, Himmelbach A, et al. A chromosome conformation capture ordered  
322 sequence of the barley genome. Nature. 2017; 544(7651): 427
- 323 16. Chin CS, Peluso P, Sedlazeck FJ et al. Phased diploid genome assembly with single molecule real-  
324 time sequencing. Nat Methods. 2016;13:1050.
- 325 17. Boetzer M, Pirovano W. SSPACE-LongRead: scaffolding bacterial draft genomes using long read  
326 sequence information. BMC Bioinf. 2014; 15(1): 211.
- 327 18. English AC, Richards S, Han Y, et al. Mind the gap: upgrading genomes with Pacific Biosciences  
328 RS long-read sequencing technology. PLoS One. 2012; 7(11): e47768.
- 329 19. Walker BJ, Abeel T, Shea T, et al. Pilon: an integrated tool for comprehensive microbial variant  
330 detection and genome assembly improvement. Plos One. 2014; 9(11): e112963.
- 331 20. Burton JN, Adey A, Patwardhan RP, et al. Chromosome-scale scaffolding of *de novo* genome  
332 assemblies based on chromatin interactions. Nat Biotechnol. 2013; 31(12): 1119–1125.
- 333 21. Jun X, Tianxing L, Qing C, et al. Karyotypes of Zhedong White Goose and Siji Goose. China Poultry.  
334 2007; 21(9): 27-29.
- 335 22. Benson G. Tandem repeats finder: a program to analyze DNA sequences. Nucleic Acids Res. 1999;  
336 27(2): 573–580.
- 337 23. RepeatMolder software. <http://www.repeatmasker.org/RepeatModeler/>.
- 338 24. Price AL , Jones NC, Pevzner PA. De novo identification of repeat families in large genomes.

339        Bioinformatics 2005;21(suppl 1):i351–8.

340    25. Price AL, Jones NC, Pevzner PA. De novo identification of repeat families in large genomes.  
341        Bioinformatics. 2005;21:i351–8. Bao W, Kojima KK, Kohany O. Repbase Update, a database of  
342        repetitive elements in eukaryotic genomes. *Mobile DNA*. 2015; 6(1):11.

343    26. Maja TG, Nansheng C. Using RepeatMasker to identify repetitive elements in genomic sequences.  
344        *Curr Protoc Bioinf*. 2009; 25(1): 4.10.11–14.10.14.

345    27. Allred DB, Cheng A, Sarikaya M, et al. . Three-dimensional architecture of inorganic nanoarrays  
346        electrodeposited through a surface-layer protein mask. *Nano Lett*. 2008;8(5):1434–8.

347    28. Burge C, Karlin S. Prediction of complete gene structures in human genomic DNA. *J Mol Biol*.  
348        1997; 268(1): 78–94.

349    29. Blanco E, Parra G, Guigó R. Using geneid to identify genes. *Curr Protoc Bioinf*. 2007; 18(1): 4.3.1-  
350        4.3.28.

351    30. Stanke M, Steinkamp R, Waack S. AUGUSTUS: a web server for gene finding in eukaryotes.  
352        *Nucleic Acids Res*. 2004; 32(suppl\_2): W309–W312.

353    31. Gertz EM, Yu YK, Agarwala R, Schäffer, A. A. & Altschul, S. F. Composition-based statistics and  
354        translated nucleotide searches: improving the TBLASTN module of BLAST. *BMC Biol*. 2006; 4(1):  
355        41.

356    32. Birney E, Clamp M, Durbin R. Gene Wise and Genomewise. *Genome Res*. 2004; 14(5): 988–995.

357    33. Grabherr MG, Haas BJ, Yassour M, et al. Full-length transcriptome assembly from RNA-Seq data  
358        without a reference genome. *Nat Biotechnol*. 2011; 29(7): 644–652.

359    34. Trapnell C, Pachter L, Salzberg SL. TopHat: discovering splice junctions with RNA-Seq.  
360        *Bioinformatics*. 2009; 25(9): 1105–1111.

- 361 35. Haas BJ, Salzberg SL, Zhu W, et al. Automated eukaryotic gene structure annotation using  
362 EvidenceModeler and the Program to Assemble Spliced Alignments. *Genome Biol.* 2008; 9(1): R7.
- 363 36. Dobin A, Davis CA, Schlesinger F, et al. STAR: ultrafast universal RNA-seq aligner. *Bioinformatics.*  
364 2013; 29(1): 15–21.
- 365 37. Trapnell C, Williams BA, Pertea G, et al. Transcript assembly and quantification by RNA-Seq  
366 reveals unannotated transcripts and isoform switching during cell differentiation. *Nat Biotechnol.*  
367 2010; 28(5): 511–515.
- 368 38. Niknafs YS, Pandian B, Iyer HK, et al. TACO produces robust multisample transcriptome  
369 assemblies from RNA-seq. *Nat Methods.* 2017; 14(1): 68.
- 370 39. Kang YJ, Yang DC, Kong L, et al. CPC2: a fast and accurate coding potential calculator based on  
371 sequence intrinsic features. *Nucleic Acids Res.* 2017; 45(W1): W12–W16.
- 372 40. Finn RD, Bateman A, Clements J, et al. Pfam: the protein families database. *Nucleic Acids Res.*  
373 2014; 42(D1): D222–D230.
- 374 41. Bateman A, Coin L, Durbin R, et al. The Pfam protein families database. *Nucleic Acids Res.* 2004;  
375 32 (suppl\_1): D138–D141.
- 376 42. Zhang G, Li C, Li Q, et al. Comparative genomics reveals insights into avian genome evolution and  
377 adaptation. *Science.* 2014; 346(6215): 1311–1320.
- 378 43. Ottenburghs J, Megens HJ, Kraus RH, et al. A history of hybrids? Genomic patterns of introgression  
379 in the True Geese. *BMC Evol Biol.* 2017; 17(1): 201.
- 380 44. Fischer S, Brunk BP, Chen F, et al. Using OrthoMCL to assign proteins to OrthoMCL- DB groups  
381 or to cluster proteomes into new ortholog groups. *Curr Protoc Bioinf.* 2011; 35(1): 6–12.
- 382 45. Stamatakis A. RAxML version 8: a tool for phylogenetic analysis and post-analysis of large

- 383 phylogenies. *Bioinformatics*. 2014; 30(9): 1312–1313.
- 384 46. Bie T, Cristianini N, Demuth J. CAFE: a computational tool for the study of gene family evolution.  
385 *Bioinformatics*. 2006; 22(10): 1269-1271.
- 386 47. Józefiak DA, Rutkowski A, Martin SA. Carbohydrate fermentation in the avian ceca: a review.  
387 *Anim Feed Sci Technol*. 2004; 113(1-4): 1-15.
- 388 48. Watanabe, YY. Flight mode affects allometry of migration range in birds. *Ecol Lett*. 2016; 19(8):  
389 907-914.
- 390 49. Yoshino H, Nishioka K, Li Y, et al. GCH1 mutations in dopa-responsive dystonia and Parkinson's  
391 disease[J]. *J Neuro*, 2018, 265(8): 1860-1870.
- 392 50. Gu Y, Lu K, Yang G, et al. Mutation spectrum of six genes in Chinese phenylketonuria patients  
393 obtained through next-generation sequencing[J]. *PLoS One*, 2014, 9(4): e94100.
- 394 51. He Y B, Duojizhuoma C Y, Cai-juan D B, et al. GCH1 plays a role in the high-altitude adaptation  
395 of Tibetans. *Zool Res*. 2017; 38(3): 155–162.
- 396 52. Verma S, De Jesus P, Chanda S K, et al. SNW1, a novel transcriptional regulator of the NF- $\kappa$ B  
397 pathway. *Mol Cell Biol*. 2019; 39(3): e00415-18.
- 398 53. Tolde O, Folk P. Stress-induced expression of p53 target genes is insensitive to SNW1/SKIP  
399 downregulation[J]. *Cell Mol Biol Lett*, 2011, 16(3): 373-384.
- 400 54. Wu M Y, Ramel M C, Howell M, et al. SNW1 is a critical regulator of spatial BMP activity, neural  
401 plate border formation, and neural crest specification in vertebrate embryos[J]. *PLoS Biol*, 2011,  
402 9(2): e1000593.
- 403 55. Huang Y H, Klingbeil O, He X Y, et al. POU2F3 is a master regulator of a tuft cell-like variant of  
404 small cell lung cancer. *Gene Dev*. 2018; 32(13-14): 915-928.

- 405 56. Matsumoto I, Ohmoto M, Narukawa M, et al. Skn-1a (Pou2f3) specifies taste receptor cell  
406 lineage[J]. Nat Neurosci, 2011, 14(6): 685.
- 407 57. Battulin N, Fishman VS, Mazur AM, et al. Comparison of the three-dimensional organization of  
408 sperm and fibroblast genomes using the Hi-C approach. Genome Biol. 2016; 17(1): 6.
- 409 58. Lieberman-Aiden E, van Berkum NL, Williams L, et al. Comprehensive mapping of long-range  
410 interactions reveals folding principles of the human genome. Science. 2009; 326(5950): 289-293.
- 411 59. Rowley MJ, Nichols MH, Lyu X, Ando-Kuri M, et al. Evolutionarily Conserved Principles Predict  
412 3D Chromatin Organization. Mol Cell. 2017; 67(5): 837-852.
- 413 60. Dixon JR, Selvaraj S, Yue F, et al. Topological domains in mammalian genomes identified by  
414 analysis of chromatin interactions. Nature. 2012; 485(7389): 376-380.
- 415 61. Ron G, Globerson Y, Moran D and Kaplan T. Promoter-enhancer interactions identified from Hi-C  
416 data using probabilistic models and hierarchical topological domains. Nat Commun. 2017; 8(1):  
417 2237.
- 418 62. Li Y, Gao G, Lin Y, Hu S, Luo Y, Wang G et al. Supporting data for "PacBio assembly with Hi-C  
419 mapping generates an improved, chromosome-level goose genome" GigaScience Database. 2020.  
420 <http://dx.doi.org/10.5524/100789>

**Table1 Summary of sequencing data for goose genome assembly.**

<b>Pair-end libraries</b>	<b>Insert size (bp)</b>	<b>Total data (Gb)</b>	<b>Read length (bp)</b>	<b>Sequence coverage (x)</b>
<b>Illumina reads</b>	350	181.52	150	141.81
<b>Pacbio reads</b>	20,000	84.31		65.86
<b>Hi-C</b>	350	149.70	150	116.95
<b>Total</b>		415.53		324.63



**Table2 Comparison of quality metrics of this study and the previous goose genome assemblies.**

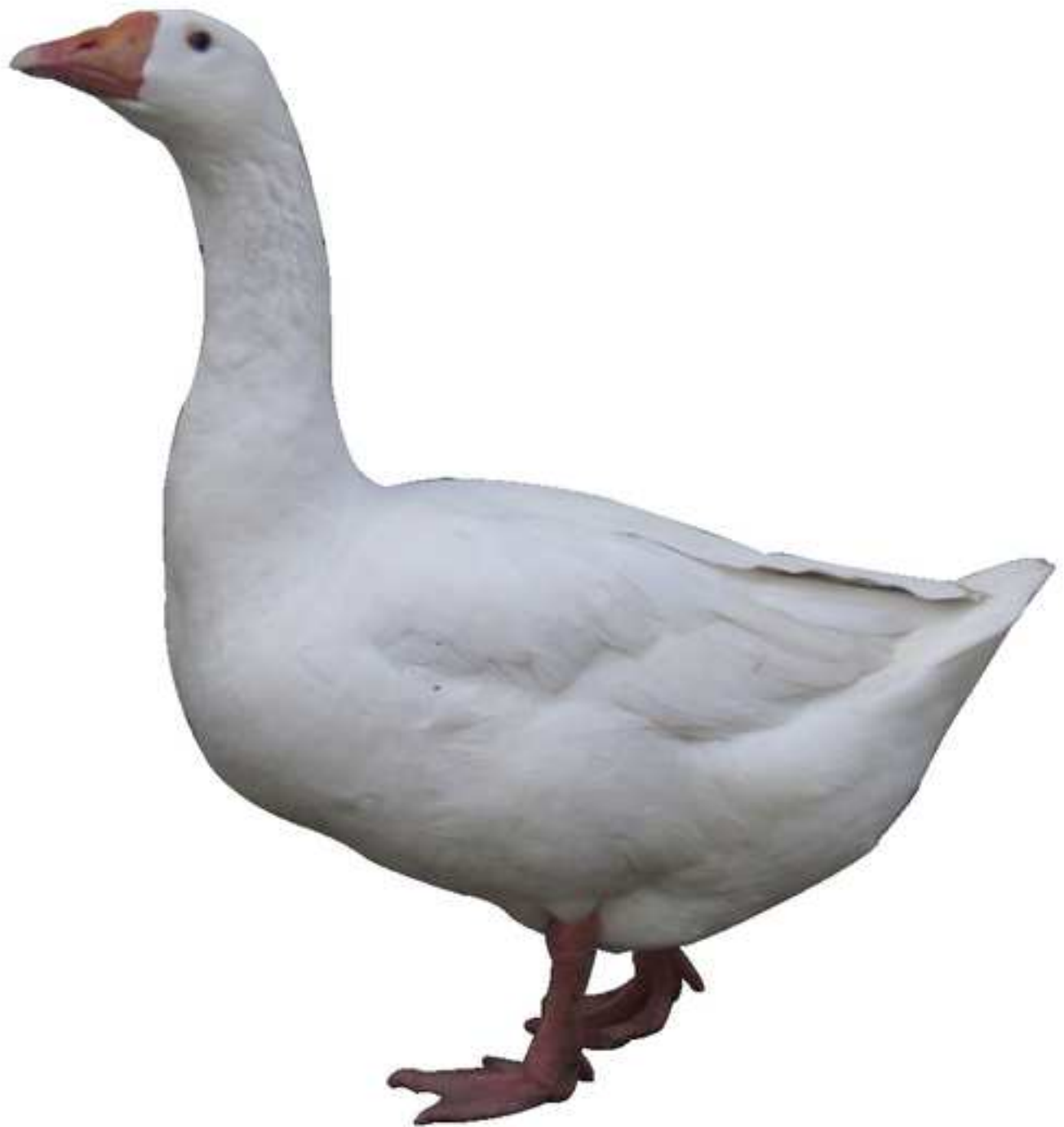
<b>Genomic features</b>	<b>This study</b>	<b>Lu <i>et al.</i><sup>a</sup></b>	<b>Gao <i>et al.</i><sup>b</sup></b>
Estimation of genome size (bp)	1,277,099,016	1,208,661,181	1,198,802,839
Total length of assembled contigs (bp)	1,113,842,245	1,086,838,604	1,100,859,441
Total size of assembled scaffolds (bp)	1,113,913,845	1,122,178,121	1,130,663,797
Number of contigs (>2kb)	2,771	60,979	53,336
Number of scaffolds (>2kb)	2,055	1,050	1,837
Contigs N50 (bp)	1,849,874	27,602	35,032
Scaffolds N50 (bp)	33,116,532	5,202,740	5,103,766
Longest contig (bp)	10,766,871	201,281	399,111
Longest scaffold (bp)	70,896,740	24,051,356	20,207,557
GC content (%)	42.15	38.00	41.68
Number of gene model	17,568	16,150	16,288
Repetitive regions percentage of genome (%)	8.67	6.33	6.90

<sup>a</sup> From the ref. 8. <sup>b</sup> From the ref. 9.

**Table 3 A comparative summary of predicted genes within each goose genome assembly.**

<b>Property</b>	<b>This study</b>	<b>Lu <i>et al.</i><sup>a</sup></b>	<b>Gao <i>et al.</i><sup>b</sup></b>
Total PCG length (bp)	326,863,440	439,289,059	500,923,091
PCG number	17,568	16,150	16,288
PCG percentage of genome (%)	29.34	39.25	44.31
Total exons number	152,392	158,713	167,532
Average exons per gene	8.67	10.92	10.29
Total exons length (bp)	26,883,354	25,763,242	26,157,477
Exons percentage of genome (%)	2.41	2.31	2.31
Average exons length (bp)	176.41	162.33	156.13
Average introns length (bp)	2224.97	2867.48	3139.07

<sup>a</sup> From the ref. 8. <sup>b</sup> From the ref. 9.



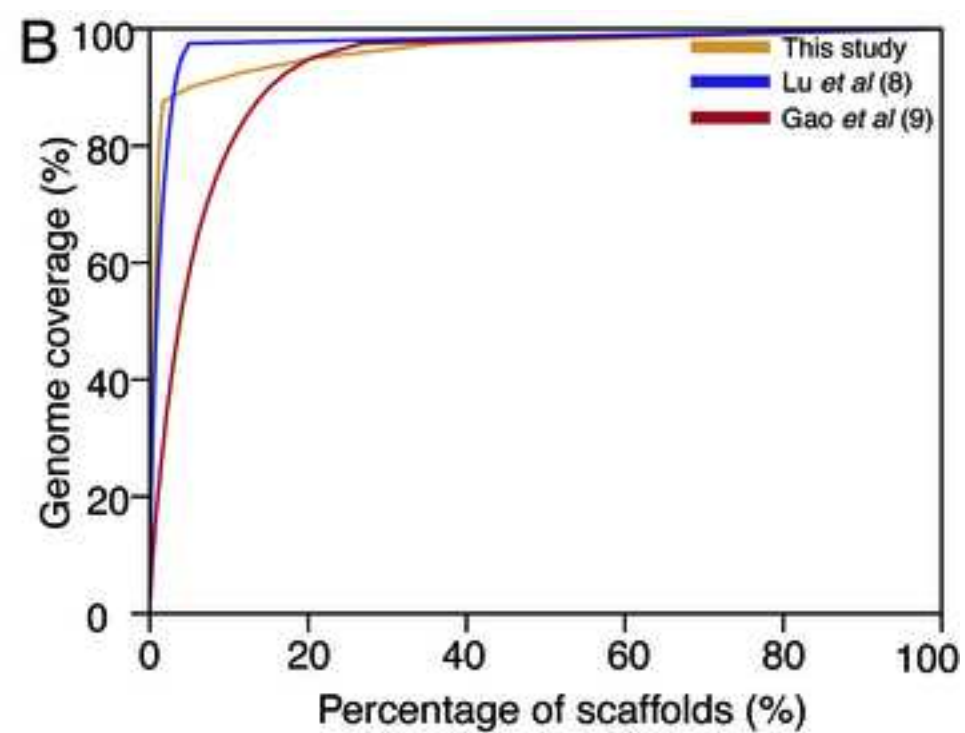
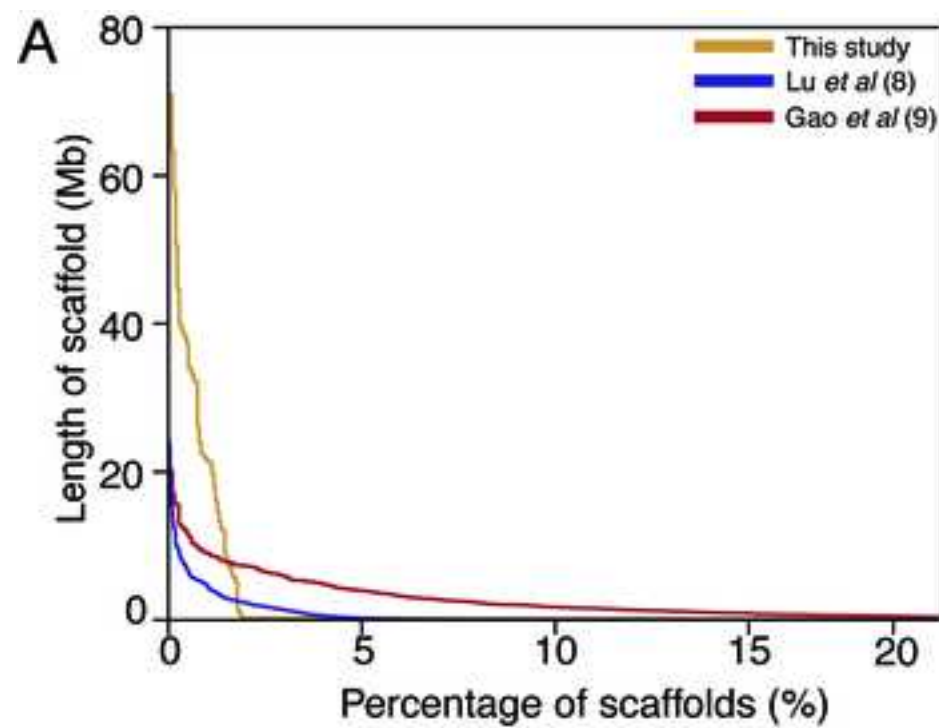
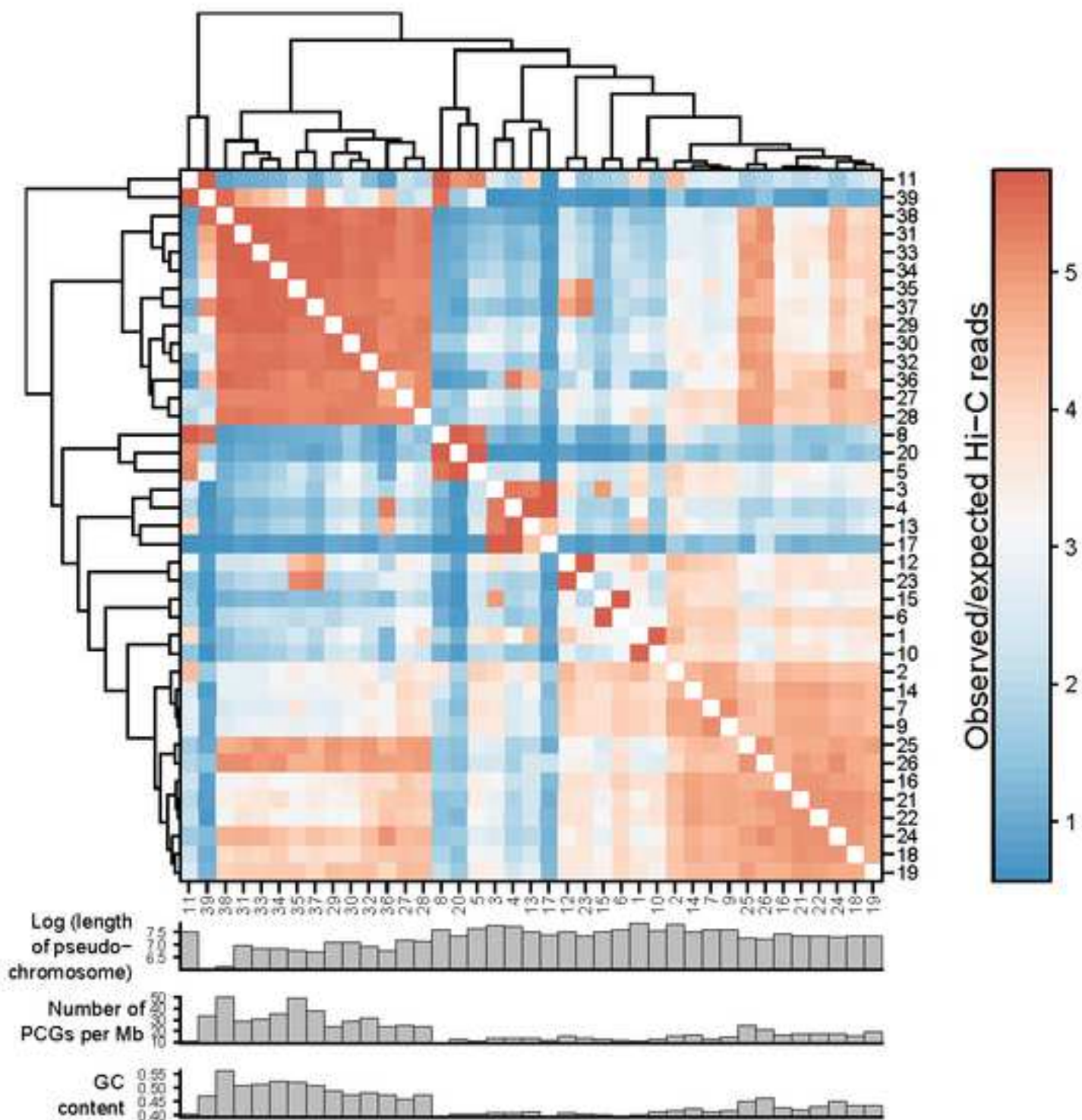
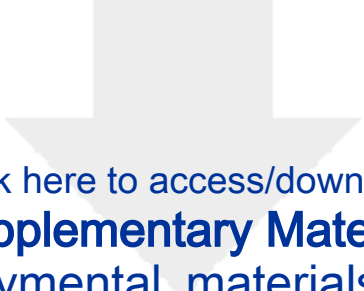


Figure 3 Dendrogram of inter-pseudo-chromosome interaction patterns generated by the average linkage algorithm.

[Click here to access/download;Figure;Figure 2u.tif](#)





Click here to access/download  
**Supplementary Material**  
Supplymental\_materials.docx

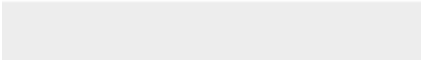

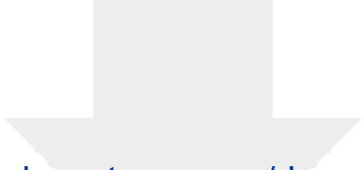


Table S1 Summary of the Pacbio initial assembly and Hi-C reads mapping used for goose genome assembly process.



Click here to access/download  
**Supplementary Material**  
Table S1.xls

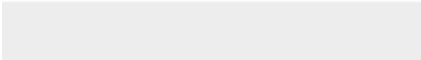

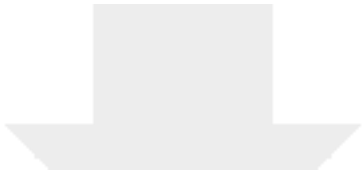


Table S2 Summary of the length of pseudo-chromosomes in  
goose genome.



Click here to access/download  
**Supplementary Material**  
Table S2.xls

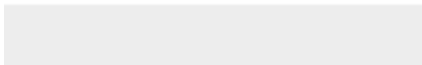
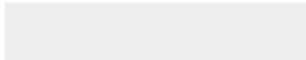
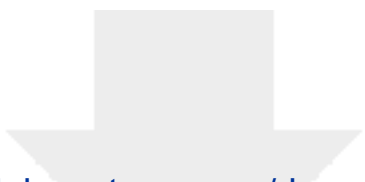




Table S3 A comparative summary of assembled repeat content between this study and previous studies.



Click here to access/download  
**Supplementary Material**  
Table S3.xls

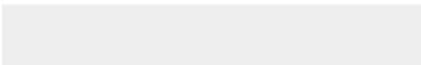

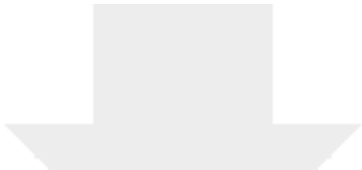


Table S4 Comparison of the mapping rates of the wild goose  
resequencing data between our goose genome and two previous



Click here to access/download  
**Supplementary Material**  
Table S4.xls

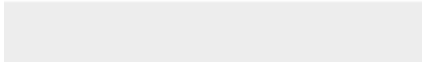

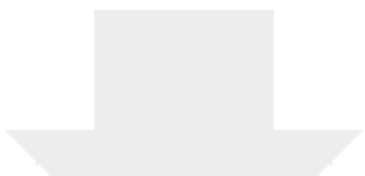


Table S5 Gene ontology (GO) enrichment analysis for the lineage-specific genes annotated in goose genome.



Click here to access/download  
**Supplementary Material**  
Table S5.xls

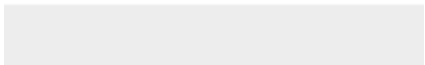

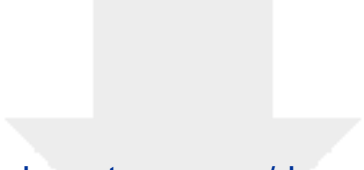


Table S6 Functional gene categories enriched for the goose  
genome-specific expansion gene families.



Click here to access/download  
**Supplementary Material**  
Table S6.xls

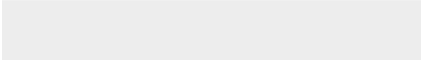

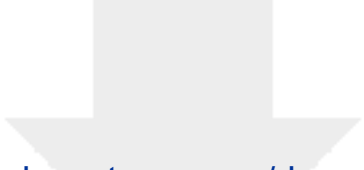


Table S7 Functional gene categories enriched for the contraction of gene families in goose genome.



Click here to access/download  
**Supplementary Material**  
Table S7.xls

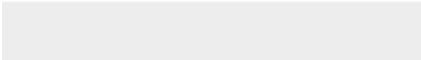




Table S8 Positively selected genes (PSGs) identified in the goose genome.



Click here to access/download  
**Supplementary Material**  
Table S8.xlsx

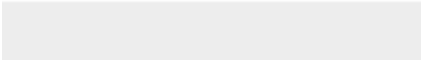





Table S9 The PC1 values (100 Kb) through Principal Component Analysis (PCA) and A-B index values (25 Kb).



Click here to access/download  
**Supplementary Material**  
Table S9.xlsx

Table S10 TAD in genome coordinates of our goose genome by using method of DI values.



Click here to access/download  
**Supplementary Material**  
Table S10.xlsx

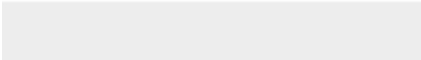






Table S11 Detailed information of promoter-enhancer interactions (PEIs) identified in goose genome.



Click here to access/download  
**Supplementary Material**  
Table S11.xlsx

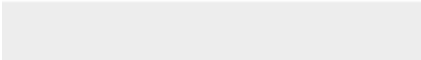




Figure S1 The Hi-C interaction contact heatmap of goose  
pseudochromosome genome assembly (bin size is 1Mb).



Click here to access/download  
**Supplementary Material**  
Figure S2u.jpg

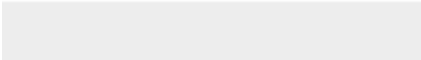




Figure S2 The shared homologous gene families across the six species (Chicken, Goose, Human, Mouse, Pig, Zebra finch).



Click here to access/download  
**Supplementary Material**  
Figure S3u.tiff

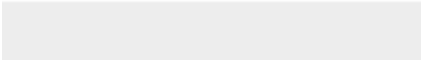

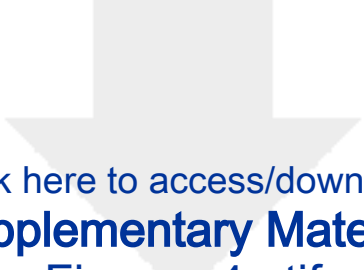


Figure S3 The distribution of gene density in the goose genome.  
Number of PCGs in each 1Mb bins was counted.



Click here to access/download  
**Supplementary Material**  
Figure s4u.tif





Figure S4 Divergence of time and the expansion, contraction gene families in the seventeen species (Ostrich, Duck, Goose, Chicken,



Click here to access/download  
**Supplementary Material**  
Figure S5.jpg

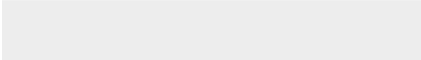




Figure S5 Resolution evaluation showing that the Hi-C data attained 2 Kb.



Click here to access/download  
**Supplementary Material**  
Figure S6.tif





Figure S6 Vioplot of PC1 values in 100 Kb bins with various number of PCGs. PC1 value indicates the chromatin activity.



Click here to access/download  
**Supplementary Material**  
Figure S7u.tif

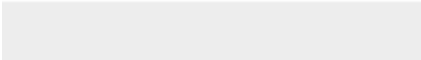

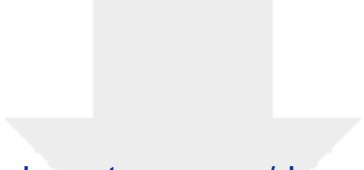
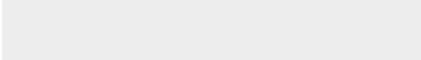




Figure S7 TPMs of PCGs located in A compartments were consistently higher than PCGs in B compartments both at 25 Kb



Click here to access/download  
**Supplementary Material**  
Figure S8u.tif







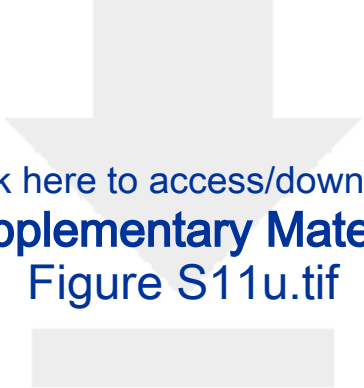
Click here to access/download  
**Supplementary Material**  
Figure S9.tif





Click here to access/download  
**Supplementary Material**  
Figure S10u.tif

Figure S10 Gene expression levels positively correlated with the number of its associated enhancers in all three liver tissues,



Click here to access/download  
**Supplementary Material**  
Figure S11u.tif